

available at www.sciencedirect.comjournal homepage: www.elsevier.com/locate/biochempharm

The anti-inflammatory actions of LCY-2-CHO, a carbazole analogue, in vascular smooth muscle cells

Feng-Ming Ho^{a,b}, Hao-Cheng Kang^c, Sho-Tone Lee^d, Yee Chao^e,
You-Ci Chen^c, Li-Jiau Huang^f, Wan-Wan Lin^{c,*}

^a Department of Internal Medicine, Tao-Yuan General Hospital Department of Health, The Executive Yuan, Tao-Yuan, Taiwan

^b Department of Biomedical Engineering, Chung Yuan Christian University, Tao-Yuan, Taiwan

^c Department of Pharmacology, College of Medicine, National Taiwan University, Taipei, Taiwan

^d Institute of Biomedical Science, Academia Sinica, Taipei, Taiwan

^e Cancer Center, Veterans General Hospital, Taipei, Taiwan

^f Department of Internal Medicine, China Medical University and Hospital, Taichung, Taiwan

ARTICLE INFO

Article history:

Received 7 March 2007

Accepted 4 April 2007

Keywords:

LCY-2-CHO

HO-1

Anti-inflammation

Cell signaling

Vascular smooth muscle

ABSTRACT

LCY-2-CHO has anti-inflammatory actions on macrophages. To understand its therapeutic implication in atherosclerosis, we examined its effects on the expressions of anti-inflammatory and inflammatory proteins in cultured rat aortic vascular smooth muscle cells (VSMC). LCY-2-CHO is able to induce heme oxygenase-1 (HO-1) protein expression through a transcriptional action. The HO-1 inducing effect of LCY-2-CHO was inhibited by SB203580, N^G-nitro-L-arginine methylester (L-NAME), and wortmannin, but was not affected by U0126 or SP600125. In accordance LCY-2-CHO increased protein phosphorylation of p38, Akt, and eNOS. Nrf2 is a transcription factor essential for HO-1 gene induction and we showed that LCY-2-CHO is able to cause Nrf2 nuclear translocation and this action depends on p38, Akt and eNOS. In addition to induce anti-inflammatory HO-1, LCY-2-CHO reduced interleukin-1 β (IL-1 β)-induced inflammatory mediators, inducible nitric oxide synthase (iNOS), cyclooxygenase-2 (COX-2), growth-related oncogene protein- α (GRO- α), and interleukin-8 (IL-8). Inhibitory effect on IL-1 β -mediated NF- κ B activation was evidenced by the diminishment of I κ B kinase (IKK) phosphorylation and I κ B α degradation. In contrast, IL-1 β -mediated ERK and JNK activations were not changed by LCY-2-CHO, while p38 activation by IL-1 β and LCY-2-CHO displayed the non-additivity. Taken together, given the overall anti-inflammatory properties of LCY-2-CHO

* Corresponding author at: Department of Pharmacology, College of Medicine, National Taiwan University, Taiwan.
Tel.: +886 2 23123456x8315; fax: +886 2 23915297.

E-mail address: wwl@ha.mc.ntu.edu.tw (W.-W. Lin).

Abbreviations: ARE, anti-oxidant response element; COX-2, cyclooxygenase-2; GRO- α , growth-related oncogene protein- α ; HO-1, heme oxygenase-1; IKK, I κ B kinase; IL-1 β , interleukin-1 β ; IL-8, interleukin-8; iNOS, inducible nitric oxide synthase; LPS, lipopolysaccharide; MAPK, mitogen-activated protein kinase; MBP, myelin basic protein; MTT, 3-(4,5-dimethylthiazol-2-yl)2,5-diphenyltetrazolium; L-NAME, N^G-nitro-L-arginine methylester; NF- κ B, nuclear factor κ B; NO, nitric oxide; PGE₂, prostaglandin E₂; PGI₂, prostaglandin I₂; PI3K, phosphoinositide 3-kinase; RT-PCR, reverse-transcription polymerase chain reaction; TNF- α , tumor necrosis factor- α ; VSMC, vascular smooth muscle cells

0006-2952/\$ – see front matter © 2007 Elsevier Inc. All rights reserved.

doi:10.1016/j.bcp.2007.04.008

in VSMC, in terms to induce HO-1 gene expression and inhibit inflammatory gene expression, these results highlight the therapeutic potential of LCY-2-CHO in atherosclerosis.

© 2007 Elsevier Inc. All rights reserved.

1. Introduction

Heme oxygenase (HO) catalyzes the rate-limiting step in the oxidative degradation of heme (a potent oxidant) to biliverdin (rapidly converted to bilirubin, an anti-oxidant), iron (sequestered by ferritin), and carbon monoxide (CO, a vasodilatory gas that has anti-inflammatory properties) [1]. Three distinct isoforms of HO (HO-1, -2, -3) were identified [2–4], while HO-3 is a pseudogene derived from HO-2 gene and has no function demonstrated thus far [5]. Unlike HO-2, HO-1 is ubiquitously distributed and strongly induced by oxidative, nitrosative, osmotic, hemodynamic, hyperthermia, and endoplasmic reticulum stress [6–8]. HO-1 has many beneficial effects, inclusive of the anti-oxidant, anti-apoptosis, and potent anti-inflammatory properties [1,3,9,10]. HO-1 also inhibits vascular smooth muscle cells (VSMC) growth, and inhibits the development of atherosclerotic lesions in apoE-deficient mice [11,12]. The absence of HO-1 exacerbates atherosclerotic lesion formation and vascular remodeling [13].

HO-1 gene expression can be induced through signaling pathways, such as mitogen-activated protein kinases (MAPKs) (ERK, JNK, p38 MAPK) [14,15], and phosphoinositide 3-kinase (PI3K)-dependent Akt [16]. It also has been reported that nitric oxide (NO) induces HO-1 gene expression in VSMC [6]. The mouse HO-1 gene contains multiple copies of anti-oxidant response element (ARE) sequences, whose necessity is a commonality in response to multiple agents in the activation of HO-1 [17]. Studies indicate that the transcription factor Nrf2 plays a critical role in ARE-dependent HO-1 gene expression [8,18,19]. Under normal conditions, Nrf2 is retained in the cytoplasm via its binding to the cytosolic protein Keap1 [20]. However, changes in cellular redox potential leads to the release of Nrf2 from Keap1 and its translocation to the nucleus and in turn heterodimerization with Maf, resulting in ARE-mediated gene transcription [18,20]. It has been proved that many protein kinases, such as p38 MAPK, JNK, ERK and PI3K/Akt are involved in the nuclear translocation and ARE transactivation of Nrf2 [16,21–24].

LCY-2-CHO ([9-(2-chlorobenzyl)-9H-carbazole-3-carbaldehyde]) was proved to have anti-inflammatory effect by directly down-regulating leukocyte functions, including the attenuation of neutrophil degranulation and superoxide anion (O_2^-) generation [25,26], and inhibition of lipopolysaccharide (LPS)-induced NO, prostaglandin E_2 (PGE₂) and tumor necrosis factor- α (TNF- α) production, accompanying transcriptional inhibition of LPS-induced inducible nitric oxide synthase (iNOS), cyclooxygenase-2 (COX-2), and pro-TNF- α protein in murine RAW264.7 macrophages [27,28]. Given that LCY-2-CHO is a novel compound with anti-inflammatory properties in macrophages, herein we attempt to explore its effects on HO-1, iNOS, COX-2, growth-related oncogene protein- α (GRO- α) and interleukin-8 (IL-8) protein

expression in rat aortic VSMC, hoping to clarify its potential therapeutic implication in cardiovascular disorders, such as atherosclerosis.

2. Materials and methods

2.1. Materials

Dulbecco's modified Eagle's medium, fetal bovine serum, penicillin, and streptomycin were obtained from Gibco BRL (Grand Island, NY, USA). [γ -³²P]ATP (5000 Ci/mmol) was obtained from NEN (Boston, MA, USA). Rabbit polyclonal anti-iNOS and anti- β -actin antibodies were purchased from Transduction Laboratories (Lexington, KY, USA). Polyclonal antibodies specific for HO-1, p38 MAPK, Akt, Nrf2, COX-2, I κ B kinase (IKK), I κ B α and lamin B were purchased from Santa Cruz Biotechnology (Santa Cruz, CA, USA). Polyclonal antibodies specific for phosphorylated p38 MAPK, phosphorylated Akt, and phosphorylated IKK α were purchased from Cell Signaling (Beverly, MA, USA). Murine IL-1 β , TNF- α , ELISA assay kits for IL-8 and GRO- α were obtained from R&D Systems (Minneapolis, MN, USA). 3-(4,5-Dimethylthiazol-2-yl)-2,5-dephenyltetrazolium (MTT), cycloheximide, actinomycin D, N(omega)-nitro-L-arginine methyl ester (L-NAME), MG132, homocysteine, and PMA were obtained from Sigma-Aldrich (St. Louis, MO, USA). LCY-2-CHO (purity > 99%) was synthesized as we previously described [30]. U0126, SB203580 and wortmannin were purchased from Calbiochem (San Diego, CA, USA). SP600125 was purchased from Tocris Cookson (Avon-mouth, UK). ELISA assay kit for PGE₂ and EIA assay kit for 6-ketoPGF1 α were purchased from Cayman Chemicals (Ann Arbor, MI, USA).

2.2. Cell culture

Rat aortic VSMC were prepared from thoracic aortas of male Wistar rats by using the collagenase digestion method and cultured in DMEM containing 10% (v/v) FBS, 100 units/ml penicillin and 100 μ g/ml streptomycin. For all experiments, rat aortic VSMC from passages 3 to 8 were used. Cells were incubated at 37 °C in a humidified atmosphere of 5% CO₂ in air.

2.3. Nitrite assay

Measurement of nitrite production as an assay of NO release was performed. Aliquots of conditioned media were mixed with an equal volume of Griess reagent [1% sulfanilamide and 0.1% N-(1-naphthyl)-ethylene-diamine in 5% phosphoric acid]. Nitrite concentrations were determined by comparison with the OD₅₅₀ using standard solutions of sodium nitrite prepared in cell culture medium.

2.4. Immunoblotting analysis

After agent treatment, the medium was aspirated. Cells were rinsed twice with ice-cold PBS, and 100 μ l of whole-cell lysis buffer (20 mM Tris-HCl, pH 7.5, 125 mM NaCl, 1% Triton X-100, 1 mM $MgCl_2$, 25 mM β -glycerophosphate, 50 mM NaF, 100 μ M Na_3VO_4 , 1 mM phenylmethylsulfonyl fluoride, 10 μ g/ml leupeptin, and 10 mg/ml aprotinin) was then added to each well. After cell harvest, cell lysates were centrifuged. Equal amounts of the soluble protein were electrophoresed on a SDS-PAGE, and transferred to a nitrocellulose membrane. Non-specific binding was blocked with TBST (50 mM Tris-HCl, pH 7.5, 150 mM NaCl, and 0.02% Tween 20) containing 5% non-fat milk for 1 h at room temperature. After immunoblotting with the first specific antibodies, membranes were washed three times with TBST and incubated with horseradish peroxidase-conjugated secondary antibody for 1 h. After three washes with TBST, the protein bands were detected with enhanced chemiluminescence detection reagent. To make sure equal amounts of sample protein were applied for electrophoresis and immunoblotting, β -actin or lamin B was used as an internal control.

2.5. Reverse transcription-polymerase chain reaction (RT-PCR)

The expression of HO-1 mRNA was determined by RT-PCR analysis. After drug treatment, cells were homogenized with 1 ml of RNazol B reagent (Invitrogen), and total RNA was extracted by acid guanidinium thiocyanate-phenol-chloroform extraction. RT was performed using StrataScript RT-PCR kit (Stratagene, La Jolla, CA, USA), and 10 μ g of total RNA was reverse transcribed to cDNA following the manufacturer's recommended procedures. RT-generated cDNA encoding HO-1 and β -actin genes were amplified using PCR. The oligonucleotide primers used correspond to the mouse HO-1 (sense: 5'-GAG AAT GCT GAG TTC ATG-3' and anti-sense: 5'-ATG TTG AGC AGG AAG GC-3'), and mouse β -actin (sense: 5'-GAC TAC CTC ATG AAG ATC CT-3' and anti-sense: 5'-CCA CAT CTG CTG GAA GGT GG-3'). PCR was performed in a final volume of 50 μ l containing TaqDNA polymerase buffer, all four dNTPs, oligonucleotide primers, TaqDNA polymerase, and RT products. After an initial denaturing for 1 min at 94 °C, 30 cycles of amplification (HO-1: 94 °C for 45 s, 55 °C for 30 s, and 72 °C for 30 s) were performed followed by a 10-min extension at 72 °C. PCR products were analyzed on 2% agarose gel. The mRNA of β -actin served as an internal control for sample loading and mRNA integrity.

2.6. Immunoprecipitation and p38 kinase assay

After stimulation cells were washed twice with ice-cold PBS, lysed in 1 ml lysis buffer and centrifuged. The supernatant was collected, and anti-p38 MAPK antibody with protein A/G-agarose beads was added, and then stored at 4 °C overnight. The immunoprecipitates were washed three times with lysis buffer and immune-complex kinase assays were performed on the antibody immunoprecipitates at 30 °C for 30 min in 20 μ l kinase reaction buffer (25 mM HEPES, pH 7.4, 20 mM $MgCl_2$, 0.1 mM Na_3VO_4 , 2 mM dithiothreitol, 100 mM ATP,

10 μ Ci [γ - ^{32}P]ATP) containing 50 μ g/ml myelin basic protein (MBP). The reaction was terminated with 5 \times Laemmli sample buffer and samples were separated on SDS-PAGE followed by autoradiography.

2.7. Preparation of nuclear extracts

Nuclear extracts from stimulated or non-stimulated cells were prepared by cell lysis followed by nuclear lysis. Cells were suspended in 30 μ l of buffer containing 10 mM HEPES, pH 7.9, 1.5 mM $MgCl_2$, 10 mM KCl, 0.5 mM dithiothreitol, and 0.2 mM phenylmethylsulfonyl fluoride; vortexed vigorously for 15 s; allowed to stand at 4 °C for 10 min; and centrifuged at 2000 rpm for 2 min. The pelleted nuclei were re-suspended in buffer containing 20 mM HEPES, pH 7.9, 25% glycerol, 420 mM NaCl, 1.5 mM $MgCl_2$, 0.2 mM EDTA, 0.5 mM dithiothreitol, and 0.2 mM phenylmethylsulfonyl fluoride for 20 min on ice, and then the lysates were centrifuged at 15,000 rpm for 2 min. The supernatants containing the solubilized nuclear proteins were stored at -70 °C until used for immunoblotting analysis of Nrf2 translocation.

2.8. PGE₂, PGI₂, IL-8 and GRO- α assays

VSMC cultured in 24-well plate were stimulated with indicated agents and cultured for different periods. PGE₂, 6-ketoPGF_{1 α} , IL-8 and GRO- α production were measured by commercial kits according to manufacturer's instruction.

2.9. Cell viability assay

Cells were seeded in 96-well plates and treated with LCY-2-CHO (1–30 μ M) for 24 h in the complete medium or serum-free medium. 3-(4,5-Dimethylthiazol-2-yl)2,5-diphenyltetrazolium bromide (MTT, 1 mg/ml) was added and incubated at 37 °C for 1 h. The formazan granules generated by the live cells were dissolved in 100% DMSO, and absorbance at 550 nm was monitored using a multiscanner enzyme-linked immunosorbent assay autoreader.

2.10. Statistical evaluation

Values are expressed as the mean \pm S.E.M. of at least three experiments. Analysis of variance (ANOVA) was used to assess the statistical significance of the differences, with a p-value of <0.05 being considered statistically significant.

3. Results

3.1. Effects of LCY-2-CHO on cell viability

Before examining the actions of LCY-2-CHO on rat VSMC, we determined the cell viability in cells treated with LCY-2-CHO for 24 h. Cell viability as assayed by MTT indicated no cell toxicity of LCY-2-CHO treatment for 24 h at concentrations up to 30 μ M in the complete culture medium. In contrast, when cells were incubated in serum-free condition, LCY-2-CHO at 30 μ M elicited 50% cell toxicity (Fig. 1). To avoid the interference with cell toxicity on specific actions of LCY-2-

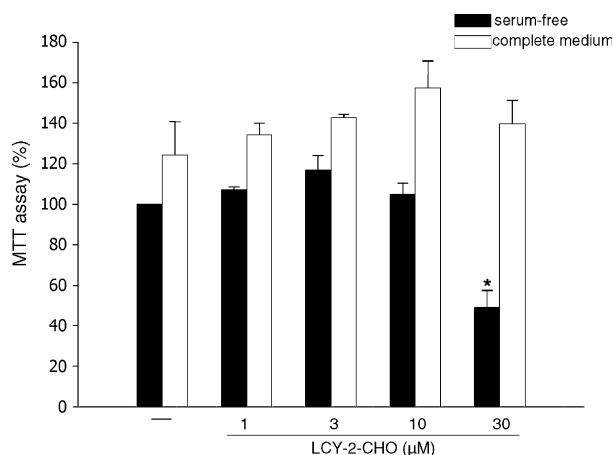


Fig. 1 – Cell viability of LCY-2-CHO-treated VSMC. Rat VSMC were treated with LCY-2-CHO for different concentrations for 24 h in the presence (complete medium) or absence (serum-free) of serum. After incubation, cells viability was determined by treating MTT. Data are mean \pm S.E.M. from three independent experiments. * $p < 0.05$, indicating significant reduction of cell viability by LCY-2-CHO.

CHO, we tested concentrations lower than 10 μ M in the following experiments.

3.2. LCY-2-CHO induces HO-1 gene expression in rat VSMC

Immunoblotting indicated that the HO-1 protein expression in VSMC 24 h following LCY-2-CHO (1–10 μ M) treatment was increased in a concentration-dependent manner (Fig. 2A). We also investigated the time-course response of HO-1 and found the increased HO-1 protein level by 10 μ M LCY-2-CHO displayed the time-dependency, occurring after 6 h exposure, peaking at 12 h and maintaining for at least 36 h (Fig. 2B). The effect of 3 μ M LCY-2-CHO, however, occurred after 12 h exposure.

Utilizing RT-PCR analysis, we found that HO-1 mRNA level was time- and concentration-dependently increased by LCY-2-CHO (Fig. 2C). The increase of HO-1 mRNA level by 10 μ M LCY-2-CHO was obvious as early as 1 h, reached the peak at 2 h and declined at 4 h. For 3 μ M LCY-2-CHO, the HO-1 mRNA induction was apparent after 4 h treatment. To further verify whether HO-1 protein expression by LCY-2-CHO results from gene transcription and consequent protein translation, we incubated cells with the transcriptional inhibitor, actinomycin

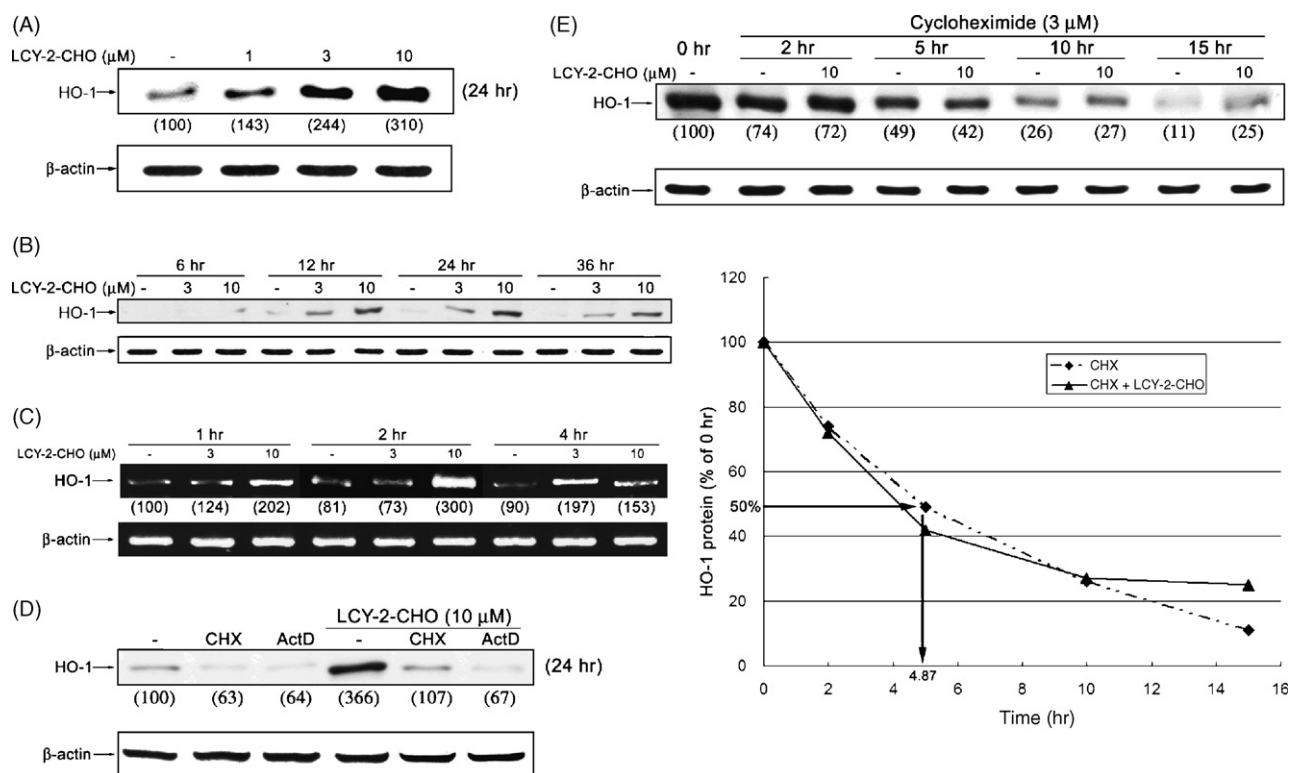


Fig. 2 – LCY-2-CHO induces HO-1 gene and protein expression in rat aortic VSMC. Rat VSMC was treated with LCY-2-CHO at concentrations indicated for different periods. After stimulation, cell lysate was prepared respectively for determining HO-1 and β -actin proteins with immunoblotting (A and B), or cell RNA was prepared for determining HO-1 and β -actin mRNA levels with RT-PCR (C). The β -actin level was considered as an internal control. Data on HO-1 protein and mRNA levels were measured by densitometry, normalized to the level of β -actin, and calculated as percentages of the control response without LCY-2-CHO treatment. In some experiments, cells were treated with cycloheximide (CHX, 3 μ M), actinomycin D (ActD, 3 μ M) and/or LCY-2-CHO (10 μ M) for 24 h (D) or for different periods (E). The stability of HO-1 protein was reflected by its half-life value (E). Traces shown are representative of three separate experiments. Numbers in parentheses are percentages of the control HO-1 protein level.

D, or the protein synthesis inhibitor, cycloheximide. Results shown in Fig. 2D confirmed this notion, as presence of either agent led to the abolishment of LCY-2-CHO response. Next, we addressed the possible action of LCY-2-CHO on the HO-1 protein stability. In condition where protein translation was blocked with cycloheximide, addition of LCY-2-CHO (10 μ M) did not alter the time-dependent decay of HO-1, which exhibited a half-life of \sim 4.8 h (Fig. 2E). These results suggest the up-regulation of HO-1 gene transcription account for the effect of LCY-2-CHO.

3.3. The HO-1 up-regulation effect of LCY-2-CHO via multiple signal pathways

Numbers of pathways have been implicated in transmitting the extracellular signals to the nuclei for HO-1 gene expression. To investigate the signal transduction pathways involved in regulating HO-1 expression of LCY-2-CHO, we used some pharmacological inhibitors of signaling intermediates and examined their effects on HO-1 protein level. As shown in Fig. 3, SB203580 (p38 MAPK inhibitor), L-NAME (NOS inhibitor), and wortmannin (PI3K inhibitor) all could attenuate the LCY-

2-CHO-induced increase in HO-1. In contrast, neither U0126 (MEK inhibitor) nor SP600125 (JNK inhibitor) could inhibit LCY-2-CHO response.

In reciprocal experiments, we found that LCY-2-CHO caused a sustained phosphorylation of p38 MAPK for at least 2 h (Fig. 4A). This action displayed the concentration-dependency at 3 and 10 μ M LCY-2-CHO, and was sensitive to the treatment with SB203580, but not to wortmannin. Akt also could be obviously phosphorylated by LCY-2-CHO addition, even though this event was transient at 30 min and could not last afterwards (Fig. 4B). The Akt phosphorylation is downstream of PI3K activation, as wortmannin treatment abrogated this action. Consistent to the established notion that Akt phosphorylation mediates eNOS phosphorylation [29], we also found eNOS phosphorylation by LCY-2-CHO, which slightly occurred at 30 min and reached obvious extent after 2 h exposure (Fig. 4C). According to the above data, we furthermore performed kinase assay to examine p38 MAPK activity. Results confirm that the LCY-2-CHO-induced phosphorylation of p38 MAPK indeed paralleled its kinase activation (Fig. 4D).

3.4. LCY-2-CHO induces Nrf2 translocation from cytosol to nuclear

According to previous studies, it has been proved that p38 MAPK and PI3K-Akt activation could respectively induce HO-1 transcriptional expression via the translocation and activation of the transcription factor Nrf2, a member of CNC-bZIP proteins, which plays a critical role in ARE-dependent HO-1 gene expression [8,17–19]. Therefore we ask whether LCY-2-CHO could also cause Nrf2 translocation from cytosol to nuclei. As shown in Fig. 5, LCY-2-CHO could rapidly and concentration-dependently induce the nuclear accumulation of Nrf2 at 30 min, as those seen in cells treated with MG132 and homocysteine. These two agents have been reported to induce HO-1 expression via Nrf2 activation [8]. Next, to understand if LCY-2-CHO-induced Nrf2 activation is related to the signaling pathways that activated by LCY-2-CHO (i.e. p38 and PI3K-Akt-eNOS), we treated cells with specific inhibitors to p38, PI3K and NOS. As a result, we found the nuclear translocation of Nrf2 was inhibited by the presence of each inhibitor (Fig. 5B).

3.5. LCY-2-CHO decreases IL-1 β -induced iNOS, COX-2, IL-8, and GRO- α protein induction

In addition to the induction of HO-1, we thereafter interested to extend LCY-2-CHO effects on IL-1 β , which is a pro-inflammatory cytokine capable of inducing inflammatory proteins, such as COX-2, iNOS, IL-8, and GRO- α . We observed that LCY-2-CHO concentration-dependently decreased the IL-1 β -induced PGE₂ (Fig. 6A) and PGI₂ production (Fig. 6B) as well as COX-2 protein expression (Fig. 6D). Moreover, IL-1 β -induced NO production (Fig. 6C) and iNOS protein expression (Fig. 6D) were likewise reduced by the presence of LCY-2-CHO. Further examining the chemokine production, data revealed that IL-8 and GRO- α release by IL-1 β were both attenuated by LCY-2-CHO within concentrations ranging 1–10 μ M (Fig. 6E and F). These findings together suggest that LCY-2-CHO has potential anti-inflammatory effects, and might have value for anti-atherosclerosis therapy.

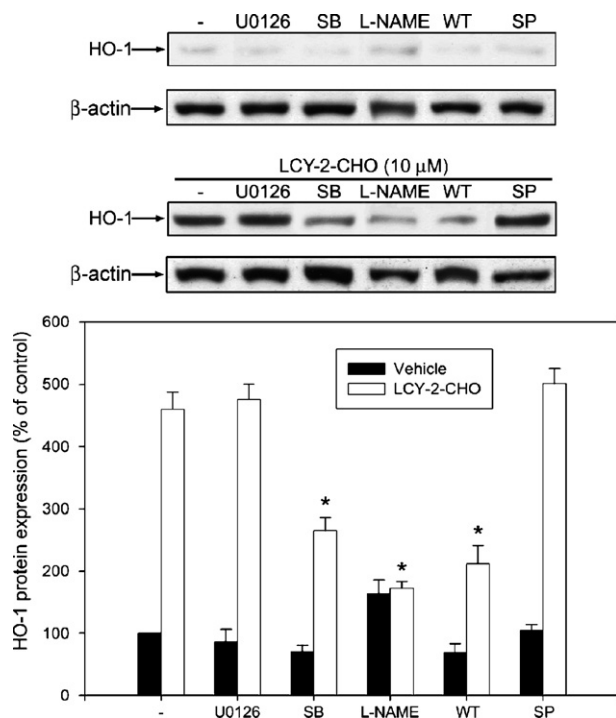


Fig. 3 – Effects of pharmacological inhibitors on LCY-2-CHO-induced HO-1 expression. Cells were pretreated with U0126 (1 μ M), SB203580 (10 μ M), L-NAME (300 μ M), wortmannin (100 nM), or SP600125 (10 μ M) for 30 min, then stimulated with LCY-2-CHO (10 μ M) for 24 h. Protein levels of HO-1 and β -actin were measured in the cell lysates by immunoblot. Data on protein levels were measured by densitometry, and calculated as percentages of the control response without agent treatment. Data are mean \pm S.E.M. from three independent experiments. * p < 0.05, indicating significant reduction of LCY-2-CHO-induced HO-1 protein expression. Traces shown are representative of three separate experiments.

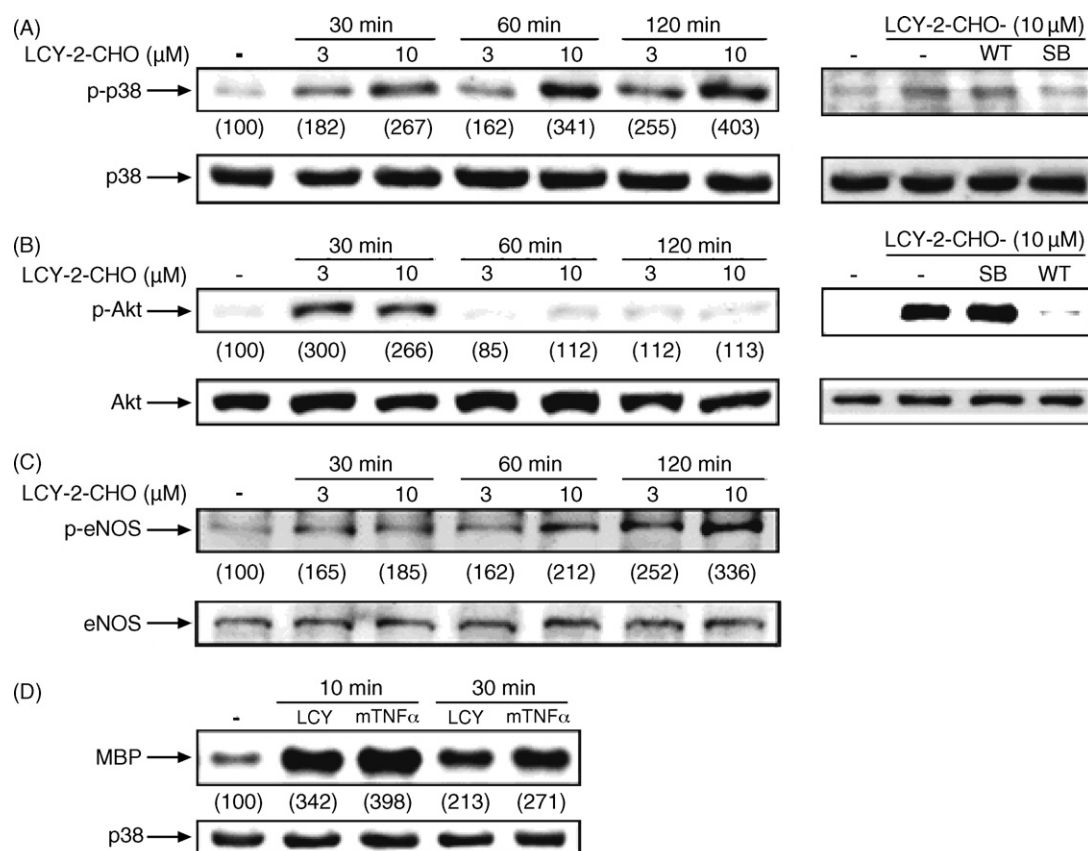


Fig. 4 – LCY-2-CHO activates p38 MAPK, Akt, and eNOS. Cell lysates prepared from cells following LCY-2-CHO (3–10 μM) stimulation for different periods were immunoblotted with antibodies specific for total or phosphorylated p38 MAPK (A), Akt (B) and eNOS (C). In some experiments, SB203580 (10 μM), L-NAME (300 μM) or wortmannin (100 nM) was pretreated for 30 min before LCY-2-CHO. In a separate experiment, cells were treated with LCY-2-CHO (10 μM) or TNF-α (50 nM) for 10 or 30 min. p38 MAPK activity was determined by immunoprecipitation and in vitro kinase assay using MBP as a substrate (D). Numbers in parentheses are percentages of the protein phosphorylation or activity as compared to cells without agent treatment. Data are representative of at least three separate experiments.

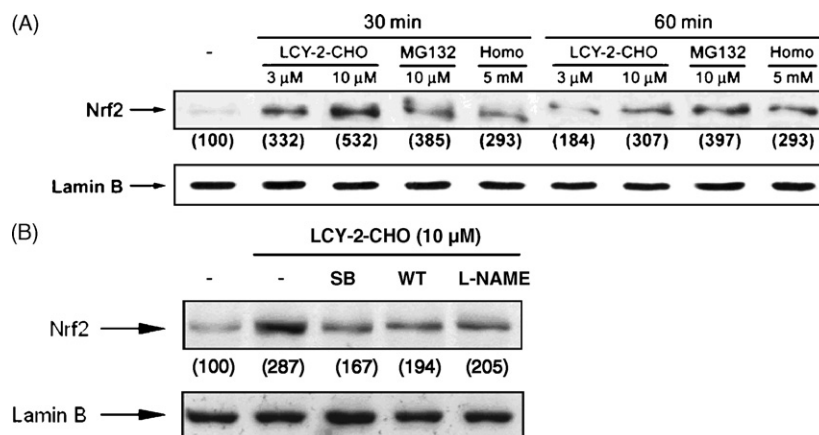


Fig. 5 – Effects of LCY-2-CHO on Nrf2 nuclear translocation. VSMC were treated with LCY-2-CHO (3–10 μM) for different periods as indicated. MG-132 and homocysteine were used as positive controls. After stimulation, nuclear protein was extracted for determining Nrf2 and lamin B with immunoblotting (A). In some experiments, SB203580 (10 μM), L-NAME (300 μM) or wortmannin (100 nM) was pretreated for 30 min before LCY-2-CHO (B). Numbers in parentheses are percentages of the protein levels as compared to cells without agent treatment. Data are representative of at least three separate experiments.

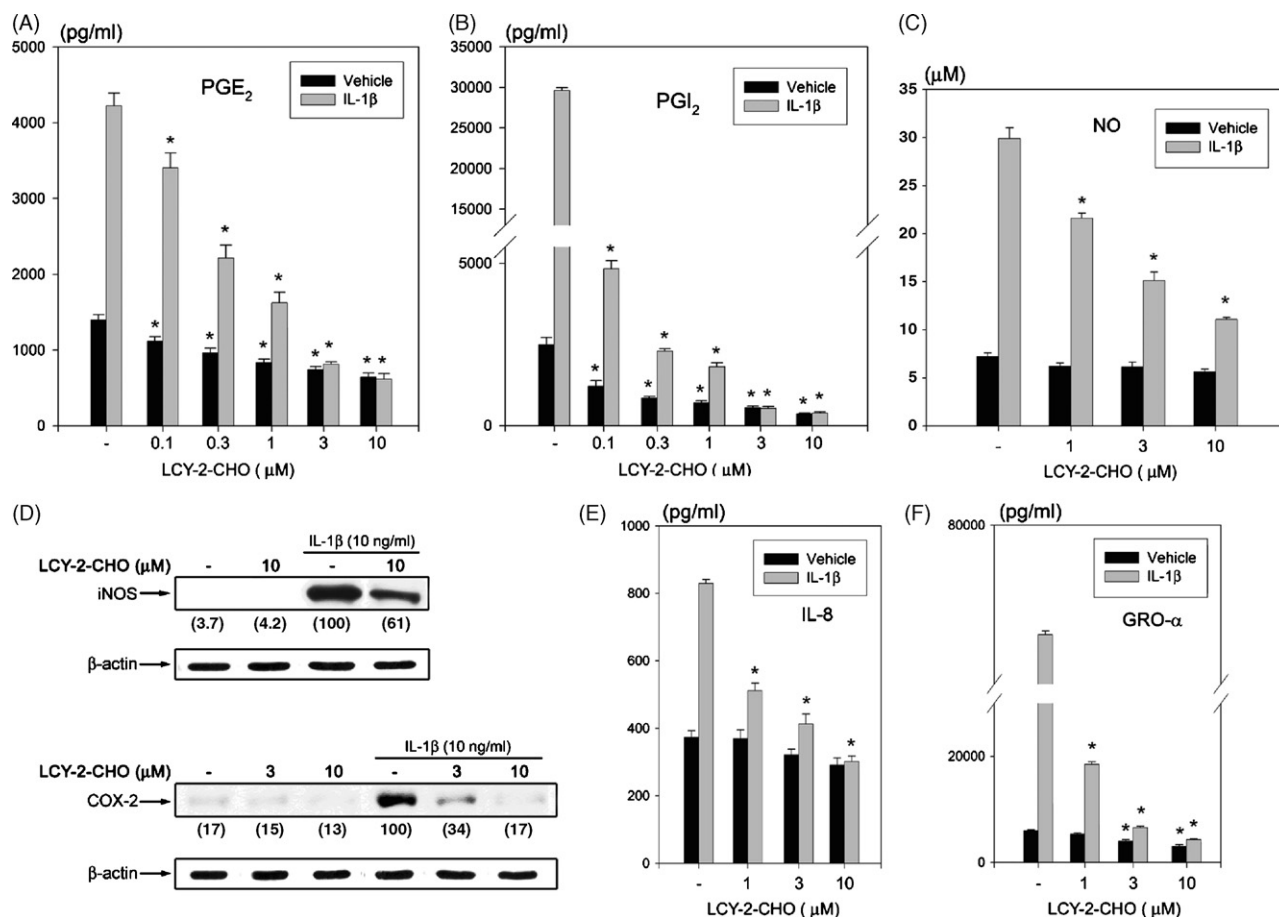


Fig. 6 – Inhibition of stimuli-induced iNOS, COX-2, IL-8 and GRO-α protein expression by LCY-2-CHO. Cells were treated with LCY-2-CHO at concentrations indicated for 30 min, and then stimulated with IL-1β (10 ng/ml) for 24 h. Medium was prepared for determining PGE₂ (A), PGI₂ (B), NO (C), IL-8 (E) and GRO-α (F) production. Protein levels of iNOS (D) and COX-2 (D) were measured in the cell lysates by immunoblot. Data are mean ± S.E.M. of at least three independent experiments. **p* < 0.05, indicating significant inhibition of mediator release as compared to the control group without LCY-2-CHO treatment. Numbers in parentheses are percentages of the protein levels as compared to cells stimulated with IL-1β alone. Traces are representative of at least three separate experiments.

3.6. LCY-2-CHO inhibits IKK activation induced by IL-1β

As NF-κB is an essential transcription factor for driving gene expression of many inflammatory proteins, we thus examined the effect of LCY-2-CHO on IL-1β-elicited IKK phosphorylation and IκBα degradation. Fig. 7A showed that IKK was rapidly phosphorylated after IL-1β stimulation. In the presence of LCY-2-CHO this action of IL-1β was reduced (Fig. 7A). Consequently, IκBα degradation occurring as early as 15 min exposure to IL-1β was inhibited and delayed by the presence of LCY-2-CHO (Fig. 7B). The inhibition of IκBα degradation by LCY-2-CHO was not affected by the treatment of SB203580, wortmannin or L-NAME, suggesting the action of LCY-2-CHO was independent of these signal pathways (Fig. 7C). In addition to inhibit IL-1β-induced NF-κB, we also examined if LCY-2-CHO affects IL-1β-induced MAPKs, thus contributing to its anti-inflammation. Results in Fig. 7D revealed that IL-1β could induce JNK, ERK and p38 activation, while LCY-2-CHO only activated p38. Neither ERK activation nor JNK activation was observed by LCY-2-CHO. Moreover, upon studying the

combinatorial effects, we found that IL-1β-induced ERK and JNK activation were not changed by LCY-2-CHO, while p38 activation exhibited the non-additivity.

4. Discussion

LCY-2-CHO has been proved to inhibit the expression of LPS-induced inflammatory mediator, such as NO, PGE₂, and TNF-α, accompanying the inhibition of LPS-induced iNOS, COX-2, and pro-TNFα proteins production in murine RAW 264.7 macrophages [27,28]. In addition, LCY-2-CHO attenuated neutrophil degranulation and superoxide anion generation, responsible for directly down-regulating leukocyte functions [25]. In the present study to further extend the therapeutic potential in cardiovascular diseases, we examined if LCY-2-CHO possesses the anti-inflammatory properties in rat VSMC. Indeed, our data demonstrate that LCY-2-CHO could decrease IL-1β-induced iNOS, COX-2, IL-8, and GRO-α protein induction in rat VSMC. Interestingly, we also found that LCY-2-CHO

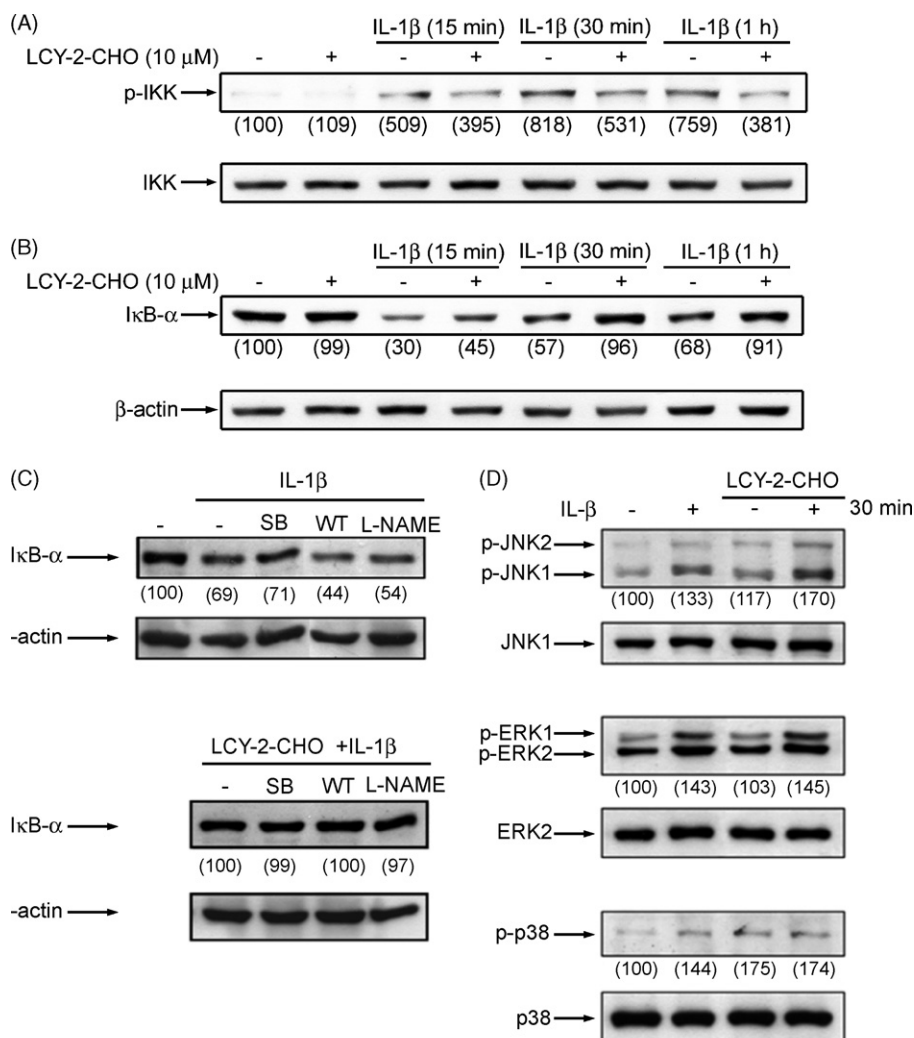


Fig. 7 – LCY-2-CHO inhibits IL-1 β -induced IKK phosphorylation and I κ B α degradation. VSMC were treated with IL-1 β (10 ng/ml) in the absence or presence of LCY-2-CHO (10 μ M) for different periods. Protein levels of phosphorylated IKK, total IKK (A), I κ B α , β -actin (B,C), JNK, ERK and p38 (D) were determined by immunoblot. In (C), SB203580 (10 μ M), L-NAME (300 μ M) or wortmannin (100 nM) was pretreated for 30 min before the co-addition of LCY-2-CHO and IL-1 β . After 30 min, immunoblotting of I κ B α was determined. Traces are representative of at least three separate experiments. Numbers in parentheses are percentages of the control protein level without agent treatment.

induces the HO-1 protein production in rat VSMC. Inducible HO-1 protein executes as a cytoprotector, which could perform the anti-oxidant, anti-apoptosis, and anti-inflammation properties [1,3,10,12,14]. In cardiovascular system, the therapeutic implication of virus-based delivering HO-1-expression has gained much attention and promising results [3,11,12]. Thus, we confirm that LCY-2-CHO, by decreasing inflammatory proteins expression and increasing HO-1 protein production, truly has the powerful anti-inflammation effect in rat VSMC.

HO-1 gene expression can be induced through signaling pathways, such as MAPKs (ERK, JNK, p38) [14,15] and PI3K-Akt [16]. Moreover, activation of p38 and PI3K could exert this action on HO-1 via the nuclear translocation and activation of transcription factor Nrf2 [8,17–19]. The nuclear translocation of Nrf2 has been demonstrated to play a key role to mediate ARE-dependent activation of the HO-1 gene [8,17–19]. Exploring the action mechanisms of LCY-2-CHO in VSMC, several

evidences in this study pointed the involvement of p38 and PI3K-Akt in a coordinative manner to mediate Nrf2 activation and consequently result in HO-1 expression. First, HO-1 induction and Nrf2 activation by LCY-2-CHO were attenuated by selective inhibitors of p38 and PI3K (SB203580 and wortmannin, respectively). In contrast, HO-1 induction was not changed by U0126 or SP600125, ruling out the participation of ERK and JNK signal pathways. Second, biochemical results confirmed that LCY-2-CHO is able to cause the active phosphorylation of p38 and Akt. In VSMC, this stimulating effect on p38 was contrast to that observed in murine macrophages where LCY-2-CHO alone failed to activate p38, but it can inhibit lipopolysaccharide-induced p38 activity [28]. These differential actions suggest the cell specific action of LCY-2-CHO. Third, LCY-2-CHO-induced signal pathways of p38 and PI3K/Akt are independent each other. All these results suggest that LCY-2-CHO-induced HO-1 expression is through

activation of p38 MAPK and PI3K-Akt, followed by increasing nuclear translocation of Nrf2, acting on ARE and inducing HO-1 gene transcription.

It has been reported that NO can induce HO-1 gene expression in VSMC [6] and other cell types [30,31]. Moreover, contribution of NO for Nrf2 activation was demonstrated [32,33]. In this study, it appears that PI3K/Akt-dependent eNOS is involved in the HO-1 induction caused by LCY-2-CHO. We found that NOS inhibitor (*L*-NAME) could reduce HO-1 protein induction and Nrf2 activation by LCY-2-CHO, and accordingly LCY-2-CHO could phosphorylate eNOS, representing the activating state. As it is quite clear that eNOS phosphorylation by Akt is essential for the enzymatic activity [29], we also examined if LCY-2-CHO-activated PI3K-Akt is the upstream signal for eNOS. As a result, we found that eNOS phosphorylation induced by LCY-2-CHO can be inhibited by wortmannin (data not shown).

In addition to induce anti-inflammatory protein HO-1, LCY-2-CHO is able to inhibit inflammatory responses of IL-1 β . In this aspect, we showed its ability to reduce several inflammatory mediators, such as iNOS, COX-2, IL-8 and GRO- α . These proteins are key mediators of many inflammatory responses, and have been implicated in the pathogenesis of atherosclerosis [34–38]. Up-regulation of IL-8 and GRO- α play a central role in macrophage recruitment and accumulation in atherosclerotic plaque [36,37]. It has been demonstrated that iNOS is present in human atherosclerotic lesions [38] and high amount of NO production from iNOS leads to tissue damage and prolonged inflammation [34]. Overexpression of COX-2 detected in symptomatic atherosclerotic plaques contributes to PGE₂-dependent plaque instability [35]. Thus, identification of these proteins as targets for prevention of atherosclerosis, as what we report for LCY-2-CHO action in this study, is promising.

When exploring the molecular mechanism for inhibition of iNOS, COX-2, IL-8 and GRO- α , we first focused on IKK-NF- κ B. The binding of NF- κ B to its specific cognate κ B sites has been shown to be functionally important for the gene transcription of these proteins [39]. Accumulating lines of evidences indicate that IKK β is a converged mediator essential for I κ B phosphorylation and proteolytic degradation. This event releases the NF- κ B dimer to translocate to the nucleus and binds DNA. In this study, we showed the ability of LCY-2-CHO to IL-1 β -induced IKK phosphorylation and subsequent I κ B α degradation in VSMC, providing additional action mechanism for the anti-inflammation property of LCY-2-CHO. Here, we do not prefer that the inhibitory action on IKK is resulting from HO-1 induction. Even though HO-1-catalyzed products (bilirubin and carbon monoxide) could interrupt IKK activation through their anti-oxidant property, the onsets of actions prompts us not to favor this possibility. LCY-2-CHO-induced HO-1 protein expression occurred after 12 h incubation, while IKK inhibition was observed at incubation periods as short as 15 min. In addition, we also showed that prevention of I κ B α degradation by LCY-2-CHO was independent of activation of p38 and PI3K/Akt/eNOS pathway.

In addition to NF- κ B, IL-1 β -activated signaling pathways might also include MAPKs and Akt [40], and account for the inflammatory responses. To elucidate if they possibly involve in the anti-inflammatory action of LCY-2-CHO, we determined

the interplay between IL-1 β and LCY-2-CHO in this aspect. We found LCY-2-CHO failed to affect ERK and JNK activation by IL-1 β . For p38, the actions of LCY-2-CHO and IL-1 β exert the non-additivity. In rat aortic VSMC stimulated with IL-1 β within 4 h, we did not detect significant Akt activation (data not shown). These results suggest that inhibitory action of LCY-2-CHO on IL-1 β -induced inflammatory mediators primarily results from the attenuation of NF- κ B, rather than MAPKs, signaling pathway.

Nrf2 is a transcription factor that is best known for providing cellular protection against oxidative insults via transcriptional activation of anti-oxidant enzymes and detoxification enzymes [22,41]. Several studies have demonstrated the prominent role of Nrf2 in anti-atherosclerosis, a disease progress comprising oxidative stress and inflammation. Nrf2/ARE pathway as an endogenous atheroprotective system for anti-oxidant protection and suppression of redox-sensitive inflammatory genes suggests that targeting the Nrf2/ARE pathway may represent a novel therapeutic approach for the treatment of atherosclerosis [42,43]. Here, we also concern if Nrf2 is a direct transcriptional regulator of iNOS, COX-2, IL-8 and GRO- α . Thus far no reports describe the direct DNA binding activity of Nrf2 on promoter regions of iNOS, IL-8 and GRO- α genes. Even though a possible ARE enhancer was identified in the COX-2 promoter, and induction of a transgene driven by the 5'-flanking region of COX-2 was increased by co-transfection with an expression vector for the Nrf2 transcription factor [44], no substantiated reports favor endogenous Nrf2/DNA binding in promoter of COX-2 gene. For IL-8 gene expression, a report showed the ability of Nrf2 to induce IL-8 and this action is mainly through mRNA stabilization instead of gene transcription [45]. Conversely, the more accepted notion is that inflammatory gene transcription might be indirectly and negatively regulated by Nrf2 through target gene products with anti-oxidant capacity and NF- κ B regulating activity [22,41,43,45,46]. Based on this notion, we cannot rule out the possibility that contribution of Nrf2 in gene transcription of iNOS, COX-2, IL-8 and GRO- α might occur at late stage through indirect induction of anti-oxidant enzymes, which balance redox state and compromise signaling pathways required for inflammatory gene transcription. Nevertheless, as mentioned previously the rapid IKK inhibition favors the suggestion that abrogation of IKK activity by LCY-2-CHO plays a major role in this event.

In summary, we have shown that in rat VSMC, LCY-2-CHO, via the ability to activate p38 MAPK, Akt, eNOS, and the translocation of Nrf2, increases the production of HO-1 protein, which has the cytoprotection, anti-inflammation and anti-atherosclerosis properties. LCY-2-CHO also can reverse the increase of pro-inflammatory proteins through the reduction of IKK-NF- κ B signaling pathway. All these results provide new evidences into the beneficial application of LCY-2-CHO in cardiovascular disorders.

Acknowledgements

This work was supported by grants from the National Science Council (NSC94-2314-B-075-005) and Academia Sinica (IBMS-CRC95-T03).

REFERENCES

- [1] Ryter SW, Otterbein LE, Morse D, Choi AM. Heme oxygenase/carbon monoxide signaling pathways: regulation and functional significance. *Mol Cell Biochem* 2002;234–235:249–63.
- [2] Maines MD, Trakshel GM, Kutty RK. Characterization of two constitutive forms of rat liver microsomal heme oxygenase. Only one molecular species of the enzyme is inducible. *J Biol Chem* 1986;261:411–9.
- [3] Maines MD. Heme oxygenase: function, multiplicity, regulatory mechanisms, and clinical applications. *FASEB J* 1988;2:2557–68.
- [4] McCoubrey Jr WK, Huang TJ, Maines MD. Isolation and characterization of a cDNA from the rat brain that encodes hemoprotein heme oxygenase-3. *Eur J Biochem* 1997;247:725–32.
- [5] Hayashi S, Omata Y, Sakamoto H, Higashimoto Y, Hara T, Sagara Y, et al. Characterization of rat heme oxygenase-3 gene. Implication of processed pseudogenes derived from heme oxygenase-2 gene. *Gene* 2004;336:241–50.
- [6] Durante W, Kroll MH, Christodoulides N, Peyton KJ, Schafer AI. Nitric oxide induces heme oxygenase-1 gene expression and carbon monoxide production in vascular smooth muscle cells. *Circ Res* 1997;80:557–64.
- [7] Tian W, Bonkovsky HL, Shibahara S, Cohen DM. Urea and hypertonicity increase expression of heme oxygenase-1 in murine renal medullary cells. *Am J Physiol Renal Physiol* 2001;281:F983–91.
- [8] Liu XM, Peyton KJ, Ensenat D, Wang H, Schafer AI, Alam J, et al. Endoplasmic reticulum stress stimulates heme oxygenase-1 gene expression in vascular smooth muscle. *J Biol Chem* 2005;280:872–7.
- [9] Otterbein LE, Choi AMK. Heme oxygenase: colors of defense against cellular stress. *Am J Physiol Lung Cell Mol Physiol* 2000;279:L1029–37.
- [10] Ishikawa K, Maruyama Y. Heme oxygenase as an intrinsic defense system in vascular wall: implication against atherogenesis. *J Atheroscler Thromb* 2001;8:63–70.
- [11] Juan SH, Lee TS, Tseng KW, Liou JY, Shyue SK, Wu KK, et al. Adenovirus-mediated heme oxygenase-1 gene transfer inhibits the development of atherosclerosis in apolipoprotein E-deficient mice. *Circulation* 2001;104:1519–25.
- [12] Durante W. Heme oxygenase-1 in growth control and its clinical application to vascular disease. *J Cell Physiol* 2003;195:373–82.
- [13] Yet SF, Layne MD, Liu X, Chen YH, Ith B, Sibinga NE, et al. Absence of heme oxygenase-1 exacerbates atherosclerotic lesion formation and vascular remodelling. *FASEB J* 2003;17:1759–61.
- [14] Immenschuh S, Ramadori G. Gene regulation of heme oxygenase-1 as a therapeutic target. *Biochem Pharmacol* 2000;60:1121–8.
- [15] Zhang X, Bedard EL, Potter R, Zhong R, Alam J, Choi AM, et al. Mitogen-activated protein kinases regulate HO-1 gene transcription after ischemia-reperfusion lung injury. *Am J Physiol Lung Cell Mol Physiol* 2002;283:L815–9.
- [16] Martin D, Rojo AI, Salinas M, Diaz R, Gallardo G, Alam J, et al. Regulation of heme oxygenase-1 expression through the phosphatidylinositol 3-kinase/Akt pathway and the Nrf2 transcription factor in response to the antioxidant phytochemical carnosol. *J Biol Chem* 2004;279:8919–29.
- [17] Gong P, Stewart D, Hu B, Vinson C, Alam J. Multiple basic-leucine zipper proteins regulate induction of the mouse heme oxygenase-1 gene by arsenite. *Arch Biochem Biophys* 2002;405:265–74.
- [18] Alam J, Wicks C, Steward D, Gong P, Touchard C, Otterbein S, et al. Mechanisms of heme oxygenase-1 gene activation by cadmium in MCF-7 mammary epithelial cells. Role of p38 kinase and Nrf2 transcription factor. *J Biol Chem* 2000;275:27694–702.
- [19] Gong P, Stewart D, Hu B, Li N, Cook J, Nel A, et al. Activation of the mouse heme oxygenase-1 gene by 15-deoxy- $\Delta(12,14)$ -prostaglandin J_2 is mediated by the stress response elements and transcription factor Nrf2. *Antioxid Redox Signal* 2002;4:249–57.
- [20] Itoh K, Wakabayashi N, Katoh Y, Ishii T, Igarashi K, Engel JD, et al. Keap1 represses nuclear activation of antioxidant responsive elements by Nrf2 through binding to the amino-terminal Neh2 domain. *Genes Dev* 1999;13:76–86.
- [21] Balogun E, Hoque M, Gong P, Killeen E, Green CJ, Foresti R, et al. Curcumin activates the haem oxygenase-1 gene via regulation of Nrf2 and the antioxidant-responsive element. *Biochem J* 2003;371:887–95.
- [22] Numazawa S, Yoshida T. Nrf2-dependent gene expressions: a molecular toxicological aspect. *J Toxicol Sci* 2004;29:81–9.
- [23] Wu CC, Hsieh CW, Lai PH, Lin JB, Liu YC, Wung BS. Upregulation of endothelial heme oxygenase-1 expression through the activation of the JNK pathway by sublethal concentrations of acrolein. *Toxicol Appl Pharmacol* 2006;214:244–52.
- [24] Wu CC, Hsu MC, Hsieh CW, Lin JB, Lai PH, Wung BS. Upregulation of heme oxygenase-1 by Epigallocatechin-3-gallate via the phosphatidylinositol 3-kinase/Akt and ERK pathways. *Life Sci* 2006;78:2889–97.
- [25] Lee CY, Huang LJ, Wang JP, Kuo SC. Anti-inflammatory activity of 9-substituted benzyl-3-substituted carbazole derivatives. *Chin Pharm J* 2002;54:35–40.
- [26] Lee CY, Kuo SC, Teng CM, Huang LJ. Synthesis and antiplatelet activity of 9-benzyl-3-hydroxymethylcarbazoles. *Chin Pharm J* 2002;54:25–34.
- [27] Tsao LT, Lee CY, Huang LJ, Kuo SC, Wang JP. Inhibition of lipopolysaccharide-stimulated nitric oxide production in RAW 264.7 macrophages by a synthetic carbazole, LCY-2-CHO. *Biochem Pharmacol* 2002;63:1961–8.
- [28] Ho FM, Lai CC, Huang LJ, Kuo TC, Chao CM, Lin WW. The anti-inflammatory carbazole, LCY-2-CHO, inhibits lipopolysaccharide-induced inflammatory mediator expression through inhibition of the p38 mitogen-activated protein kinase signaling pathway in macrophages. *Br J Pharmacol* 2004;141:1037–47.
- [29] Boo YC, Jo H. Flow-dependent regulation of endothelial nitric oxide synthase: role of protein kinases. *Am J Physiol Cell Physiol* 2003;285:C499–508.
- [30] Hara E, Takahashi K, Takeda K, Nakayama M, Yoshizawa M, Fujita H, et al. Induction of heme oxygenase-1 as a response in sensing the signals evoked by distinct nitric oxide donors. *Biochem Pharmacol* 1999;58:227–36.
- [31] Motterlini R, Foresti R, Bassi R, Calabrese V, Clark JE, Green CJ. Endothelial heme oxygenase-1 induction by hypoxia. Modulation by inducible nitric-oxide synthase and S-nitrosothiols. *J Biol Chem* 2000;275:13613–20.
- [32] Buckley BJ, Marshall ZM, Whorton AR. Nitric oxide stimulates Nrf2 nuclear translocation in vascular endothelium. *Biochem Biophys Res Commun* 2003;307:973–9.
- [33] Park EY, Kim SG. NO signaling in ARE-mediated gene expression. *Methods Enzymol* 2005;396:341–9.
- [34] Behr D, Rupin A, Fabiani JN, Verbeuren TJ. Distribution and prevalence of inducible nitric oxide synthase in atherosclerotic vessels of long-term cholesterol-fed rabbits. *Atherosclerosis* 1999;142:335–44.
- [35] Cipollone F, Prontera C, Pini B, Marini M, Fazia M, Cesare DD, et al. Overexpression of functionally coupled

- cyclooxygenase-2 and prostaglandin E synthase in symptomatic atherosclerotic plaques as a basis of prostaglandin E₂-dependent plaque instability. *Circulation* 2001;104:921–7.
- [36] Hansson GK. Immune mechanisms in atherosclerosis. *Atheroscler Thromb Vasc Biol* 2001;21:1876–90.
- [37] Boisvert WA, Rose DM, Johnson KA, Fuentes ME, Lira SA, Curtiss LK, et al. Up-regulated expression of the CXCR2 ligand KC/GRO- α in atherosclerotic lesions plays a central role in macrophage accumulation and lesion progression. *Am J Pathol* 2006;168:1385–95.
- [38] Luoma JS, Ylä-Herttuala S. Expression of inducible nitric oxide synthase in macrophages and smooth muscle cells in various types of human atherosclerotic lesions. *Virchows Arch* 1999;434:561–8.
- [39] Karin M, Ben-Neriah Y. Phosphorylation meets ubiquitination: the control of NF- κ B activity. *Annu Rev Immunol* 2000;18:621–63.
- [40] Issa R, Xie S, Lee KY, Stanbridge RD, Bhavsar P, Sukkar MB, et al. GRO- α regulation in airway smooth muscle by IL-1 β and TNF- α : role of NF- κ B and MAP kinases. *Am J Physiol Lung Cell Mol Physiol* 2006;291:L66–74.
- [41] Cho HY, Reddy SP, Kleeberger SR. Nrf2 defends the lung from oxidative stress. *Antioxid Redox Signal* 2006;8:76–87.
- [42] Hosoya T, Maruyama A, Kang MI, Kawatani Y, Shibata T, Uchida K, et al. Differential responses of the Nrf2-Keap1 system to laminar and oscillatory shear stresses in endothelial cells. *J Biol Chem* 2005;280:27244–50.
- [43] Chen XL, Dodd G, Thomas S, Zhang X, Wasserman MA, Rovin BH, et al. Activation of Nrf2/ARE pathway protects endothelial cells from oxidant injury and inhibits inflammatory gene expression. *Am J Physiol Heart Circ Physiol* 2006;290:H1862–70.
- [44] Sherratt PJ, McLellan LI, Hayes JD. Positive and negative regulation of prostaglandin E2 biosynthesis in human colorectal carcinoma cells by cancer chemopreventive agents. *Biochem Pharmacol* 2003;66:51–61.
- [45] Zhang X, Chen X, Song H, Chen HZ, Rovin BH. Activation of the Nrf2/antioxidant response pathway increases IL-8 expression. *Eur J Immunol* 2005;35:3258–67.
- [46] Yang H, Magilnick N, Lee C, Kalmaz D, Ou X, Chan JY, et al. Nrf1 and Nrf2 regulate rat glutamate-cysteine ligase catalytic subunit transcription indirectly via NF- κ B and AP-1. *Mol Cell Biol* 2005;25:5933–46.